MMT OBSERVATIONS OF THE BLACK HOLE CANDIDATE XTE J1118+480 NEAR AND IN QUIESCENCE[1]

M. A. P. Torres,[2,3] P. J. Callanan,[2] M. R. Garcia,[3] P. Zhao,[3] S. Laycock,[3] AND A. K. H. Kong[3]

ABSTRACT

We report on the analysis of new and previously published MMT optical spectra of the black hole binary XTE J1118+480 during the decline from the 2000 outburst to true quiescence. From cross-correlation with template stars, we measure the radial velocity of the secondary to derive a new spectroscopic ephemeris. The observations acquired during approach to quiescence confirm the earlier reported modulation in the centroid of the double-peaked Hα emission line. In addition, our data combined with the results presented by Zurita et al. (2002) provide support for a modulation with a periodicity in agreement with the expected precession period of the accretion disk of ∼52 days. Doppler images during the decline phase of the Hα emission line show evidence for a hot spot and emission from the gas stream: the hot spot is observed to vary its position, which may be due to the precession of the disk. The data available during quiescence show that the centroid of the Hα emission line is offset by about −100 km s^{-1} from the systemic velocity, which suggests that the disk continues to precess. An Hα tomogram reveals emission from near the donor star after subtraction of the ringlike contribution from the accretion disk, which we attribute to chromospheric emission. No hot spot is present, suggesting that accretion from the secondary has stopped (or decreased significantly) during quiescence. Finally, a comparison is made with the black hole XRN GRO J0422+32: we show that the Hα profile of this system also exhibits a behavior consistent with a precessing disk.

Subject headings: accretion, accretion disks — binaries: close — stars: individual (XTE J1118+480) — X-rays: stars

Online material: color figures

1. INTRODUCTION

Low-mass X-ray binaries (LMXBs) are binary systems in which mass from a low-mass secondary ($M_2 \lesssim 1\ M_\odot$) is accreted onto a neutron star or black hole primary via an accretion disk. A subclass of LMXBs undergo episodic outbursts, separated by periods of relatively low X-ray brightness, during which the X-ray luminosity can increase by as much as a factor of 10^7. Known as X-ray novae (XRNe), these LMXBs have provided us with some of the most secure dynamically confirmed stellar black holes. For a review of the observational and theoretical status of LMXBs, and in particular XRNe, see van Paradijs & McClintock (1995), Tanaka & Shibazaki (1996), van Paradijs (1998), and McClintock & Remillard (2004).

XTE J1118+480 is the first identified black hole XRN located in the Galactic halo (Wagner et al. 2001; Mirabel et al. 2001). After its discovery during a faint (39 mcrab) X-ray outburst in 2000 March (Remillard et al. 2000), its optical counterpart was quickly identified with a 12.9 mag emission-line object that had brightened by ∼6 mag from its pre-outburst value (Uemura et al. 2000a; Garcia et al. 2000). The multiwavelength outburst spectrum of XTE J1118+480 has been intensively studied (Hynes et al. 2000; McClintock et al. 2001a; Frontera et al. 2003). In particular, thanks to the location of XTE J1118+480 close to the Lockman Hole, it was possible to carry out observations in the extreme UV (Hynes

et al. 2000), a wavelength range inaccessible for the low Galactic latitude XRNe.

Optical photometry performed during outburst revealed a periodicity of 0.17078 days (Uemura et al. 2000b), which was later shown to be the superhump period caused by the precession of an eccentric accretion disk. During the decay of the outburst, McClintock et al. (2001b) and Wagner et al. (2001) measured the radial velocity curve of the companion star, yielding a mass function of ∼6 $M_\odot$. This is beyond the maximum allowed mass for a neutron star (Rhodes & Ruffini 1974), a result that establishes the dynamical evidence for a black hole primary in XTE J1118+480. They also found that the XRN is at a distance of 1.8 ± 0.6 kpc and has a high inclination ($i \sim 80°$) relative to the observer. Subsequent spectroscopy has refined the classification of the secondary to a probable metal-poor K5–7 V subdwarf (McClintock et al. 2003). In addition, the outburst UV emission-line spectrum showed evidence for a nuclear-evolved donor star (Haswell et al. 2002). The mean rotational broadening of the secondary yields a mass ratio of $q = M_2/M_1 = 0.037 \pm 0.007$ (Orosz 2001), which implies that the 3 : 2 resonant radius is within the disk tidal radius (see Whitehurst & King 1991 and references therein). Near quiescence, the optical light curves displayed features characteristic of the ellipsoidal variations of the secondary star (McClintock et al. 2001b; Wagner et al. 2001). A 12 minute offset between the spectroscopic and photometric ephemerides was also observed and tentatively explained by Wagner et al. as due to an asymmetrically emitting disk component. This hypothesis was confirmed by the observations of Zurita et al. (2002), who found a superhump component with a period 0.3% longer than the orbital period in their optical light curves obtained near quiescence. This superhump period implies a 52 day precession period for the accretion disk.

TABLE 1
JOURNAL OF OBSERVATIONS

Date (UT)	Number of Spectra	Exposure Time (s)	HJD Start (+2,451,000.0)	HJD End (+2,451,000.0)	λ Range (Å)
2000 Dec 1	2	900	880.0097	880.0224	3650–6825
2000 Dec 4	6	900–1200	882.5471	882.9630	3940–7120
2000 Dec 24	6	1200	902.8517	902.9851	4100–7015
2000 Dec 28	3	1100–1200	907.0248	907.0543	4090–7005
2000 Dec 29	13	1200	907.8632	908.0551	4085–7000
2001 Jan 26..........	38	600	935.7534	936.0420	4075–6990
2001 Mar 26	2	1200	994.7991	994.8147	3715–8510
2003 Jan 2............	8	900	1,641.9798	1,642.0635	4925–6850
2003 Jan 3............	9	900	1,642.9625	1,643.0581	4930–6860

In a previous paper, Torres et al. (2002b) presented the results of the analysis of their multiepoch spectroscopy following the 2000 March outburst. They reported variations in the double-peaked emission lines on a timescale longer than the orbital period of the system. This was interpreted as evidence for the precession of an elliptical accretion disk. During the approach of the system to quiescence, Zurita et al. (2002) found asymmetries in the Hα line and long-term variations in the centroid of the line, which could also be consistent with a precessing accretion disk. Simulations of emission lines arising from an eccentric precessing disk strongly support this interpretation (Foulkes et al. 2004).

In this paper we reanalyze previously published data and present new optical spectroscopy of XTE J1118+480, with the aim of studying and resolving the complex structure of the emission-line profiles. The observations comprise data acquired at a similar time to those presented in Zurita et al. (2002) and a data set acquired 550 days after the system entered quiescence. The paper is structured as follows: Section 2 presents the observations and the data reduction procedure. In § 3 we determine the orbital ephemeris and in § 4 discuss the spectrum of the donor star. Sections 5 and 6 describe the results obtained from the analysis of the Balmer emission lines. Finally, in § 7 we discuss our results, and a summary is given in § 8.

2. OBSERVATIONS AND DATA REDUCTION

We observed XTE J1118+480 with the Blue Channel CCD spectrograph attached to the 6.5 m MMT at the F. L. Whipple Observatory. All the spectra were acquired with the Loral 3072×1024 CCD binned by two in the spatial direction. Other details of the observations are summarized in Table 1.

On six nights during the period 2000 December 1 to 2001 January 26 UT we used a 500 groove mm^{-1} grating and a 1″25 slit width, which yielded a dispersion of 1.18 Å pixel^{-1} and a spectral resolution of 3.6 Å FWHM. On the night of 2001 March 26 we made use instead of a 300 groove mm^{-1} grating and a 1″ slit, which provided a dispersion of 1.94 Å pixel^{-1} and a resolution of 5.5 Å FWHM. The source visual brightness at the beginning of the observations was $R \sim 18.2$, and it continued to fade at a rate of 0.003 mag day^{-1} (Zurita et al. 2002). Some results obtained from the data acquired during the first two nights can be found in McClintock et al. (2001b). A final observing run took place on 2003 January 2/3 at a time when the system was in true quiescence ($R = 18.6$). Spectra were acquired using an 832 groove mm^{-1} grating and a 1″25 slit. This combination gave a dispersion of 0.72 Å pixel^{-1} and a resolution of 2.4 Å FWHM.

The images were bias- and flat field–corrected with standard IRAF[4] routines. Spectra were extracted with the IRAF KPNOSLIT package. HeNeAr arc lamp exposures taken regularly during the observations allowed us to derive the pixel-to-wavelength calibration. This was obtained from cubic spline fits to about 30 arc lines, giving an rms deviation of typically $\leq$0.07 Å. The wavelength scales of neighboring arc spectra were interpolated in time, and the whole process was checked and corrected by using the atmospheric [O I] 5577.34 Å sky line, which showed an rms scatter of $\leq$9 km s^{-1} per night. Except on 2003 January 2/3, spectra of flux standards were acquired throughout the observations and used to correct the target spectra for the instrumental response.

3. RADIAL VELOCITY CURVE AND ORBITAL EPHEMERIS

We extracted the radial velocities by cross-correlating each target spectrum with archival spectra of six template stars with spectral types ranging from G8 V to M0 V and acquired using the same setup as for the target (see McClintock et al. 2001b). Prior to the cross-correlation, the target and template spectra were resampled into a common logarithmic wavelength scale and normalized by dividing with the result of fitting a low-order spline to the continuum (after masking the emission lines in the target spectra). Cross-correlation was carried out in the range $\lambda\lambda$4900–6500, and least-squares sine fits with all parameters free were performed for the radial velocity determinations. Unreliable velocities obtained from two spectra were not included in these fits. We have adopted the K0 V parameters of the radial velocity curve, because it provided the lowest reduced χ^2 (3.0) for the fit $\gamma = 16 \pm 6$ km s^{-1}, $K_2 = 709 \pm 7$ km s^{-1}, $P = 0.1699339 \pm 0.0000002$ days, and $T_0 =$ HJD 2451880.1086 $\pm$ 0.0004, with T_0 corresponding to the time of closest approach of the secondary to the observer. All quoted uncertainties are 1 σ and were obtained after increasing the error in the radial velocities in order to give $\chi_{\nu}^2 = 1$. Figure 1 displays the phase-folded radial velocity curve. Our spectroscopic orbital period disagrees somewhat (at the 3 σ level) with the photometric orbital period $P_{ph} = 0.169937 \pm 0.000001$ days found by Zurita et al. (2002). Adopting the values of K_2 and the orbital period, a refined mass function of $f(M) = 6.3 \pm 0.2\ M_{\odot}$ is obtained. Finally, note that by using the above refined ephemeris the outburst Doppler maps in Torres et al. (2002b) should be rotated clockwise by $4° \pm 1°$, whereas for the tomograms presented in this paper the

---

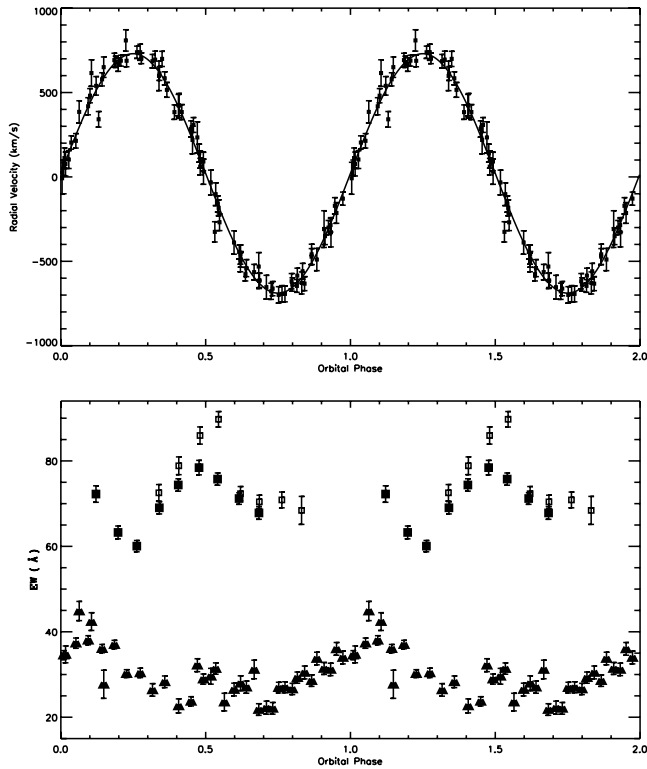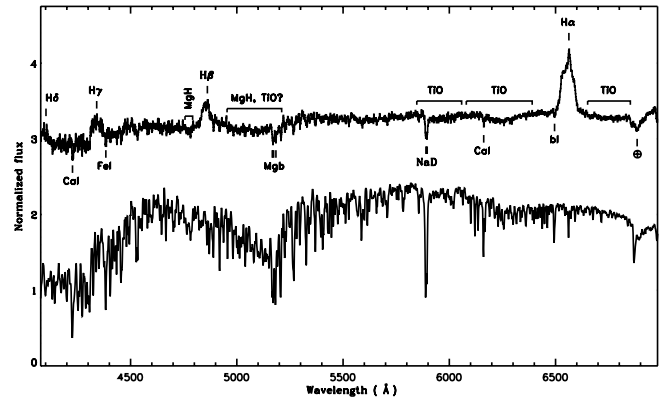[4] IRAF is distributed by the National Optical Astronomy Observatories.

FIG. 2.—Average optical MMT spectrum of XTE J1118+480 on 2001 January 26 (UT), together with the spectrum of a K8/5 V template. The spectra have been normalized at $\lambda4100$ and the spectrum of XTE J1118+480 has been shifted vertically by +2 for the sake of clarity. Major features are identified. The Earth symbol denotes the atmospheric features and *bl* the metallic blend.

FIG. 1.—*Top*: Total of 85 radial velocities of the secondary star in XTE J1118+480 folded on the ephemeris of § 3. The best-fit sine wave is also shown. *Bottom*: EWs of Hα vs. orbital phase for 2001 January 26 (*triangles*), 2003 January 2 (*open squares*), and 2003 January 3 (*filled squares*).

error offsets are negligible for the first two and within 2° for the latter.

4. THE SPECTRUM OF THE DONOR STAR

Figure 2 presents the spectrum of XTE J1118+480 for 2001 January 26. It was obtained by adding the spectra with different weights to maximize the signal-to-noise ratio after Doppler-correcting them to the rest frame of the secondary. By doing this, it is possible to see the absorption features from the companion star that would otherwise be blurred by the orbital motion of the star. As in McClintock et al. (2001b) and Wagner et al. (2001), the two strongest photospheric features detected are the NaD I doublet and the discontinuity in the continuum at $\lambda5200$ caused by the Mg *b* triplet, MgH, and (probably) the TiOα system. Also visible are the MgH band at $\lambda4780$ and the molecular bands of the TiOγ′ system situated longward of 5840 Å. Metallic features, such as the Ca I $\lambda\lambda4227, 6162$, Fe I $\lambda4384$, and the blend of chiefly Fe I+Ca I at $\lambda6495$, are also present. The molecular bands and lines from neutral elements identified are characteristic of spectral types K and M. The spectrum is bluer and the absorption features weaker relative to the K5/8 V template shown in the same figure. This is due to the continuum excess from the accretion disk. In this regard, the contribution of light from the donor star is ~35% ± 8% at $\lambda\lambda5800–6400$ on 2000 December 29 and 2001 January 26 and 60% ± 10% on 2003 January 2/3. These estimations were obtained by performing the standard optimal subtraction technique (Marsh et al. 1994) with K5–M0 dwarf templates. This is comparable to values found by other authors. In particular, the relative contribution of the secondary was found to be 53% ± 7% on 2001 April (Zurita et al. 2002) and 45% ± 10% on 2002 January (McClintock et al. 2003). These

two numbers along with ours from 2003 January are all consistent with a constant ~55% contribution from the secondary and indicate that XTE J1118+480 has reached true quiescence on these dates. Finally, there is no clear evidence in the night-averaged spectra for absorption from the Li I $\lambda6708$ resonance line to an equivalent width (EW) upper limit of 0.12 Å (1 σ) relative to the observed continuum. In comparison, strong Li I has been detected unequivocally in the companions of other XRNe. The reader should refer to Martín et al. (1994, 1996) for a discussion of the possible cause of the anomalously high abundance of Li I in XRNe.

5. THE AVERAGED EMISSION-LINE SPECTRUM

Apart from the late-type companion spectrum, Balmer lines up to Hδ in pure emission are detected in our spectra. He I and Fe II emission lines (commonly observed in XRNe and DNe in quiescence) are not discernible, although it has been shown that at least He I $\lambda5876$ is present in the spectrum of XTE J1118+480 but veiled by the continuum from the companion star (McClintock et al. 2003). In order to study the Balmer line profiles, we averaged the spectra in the observer's rest frame for the nights when six or more spectra were acquired. The line profiles have an FWHM of ~2500 km s^{-1} and appear double-peaked, a profile shape that is indicative of emission arising from an accretion disk. Table 2 presents the measured full width at zero intensity (FWZI) and EWs for the lines. In Table 3 we give the position of the peaks for Hα obtained by fitting the averaged line profiles with a three-Gaussian function, with one used to account for the base of the line and the other two for the narrow peaks in the line. In addition, their difference (peak-to-peak separation) and mean (centroid of the line) are listed. From Table 2 it is obvious that the EWs measured for Hα during 2003 January 2/3 are higher than during approach to quiescence. This is caused in part by the lower contribution from the accretion disk to the optical continuum during quiescence (§ 4). Based on Table 3, there is no evidence for a change in the peak-to-peak separation during the period of our observations, which has a weighted mean value of 1780 km s^{-1} and an rms scatter of 60 km s^{-1}. Instead, during the approach of XTE J1118+480 to quiescence, the position of the centroid of the line with respect to the rest wavelength varies noticeably from night to night with an amplitude of 250 km s^{-1}. The centroid also shows displacements

TABLE 2
FWZI and Equivalent Widths for the Balmer Lines

Date (UT)	Hα		Hβ		Hγ		Hδ	
	FWZI	EW	FWZI	EW	FWZI	EW	FWZI	EW
2000 Dec 4	88 ± 5	−22 ± 2	46 ± 10	−8 ± 2	78 ± 5	−13 ± 5	70 ± 5	−12 ± 10
2000 Dec 24	78 ± 5	−27 ± 5	55 ± 6	−12 ± 3	60 ± 5	−9 ± 3	...	...
2000 Dec 29	85 ± 6	−26 ± 4	65 ± 10	−7 ± 3	76 ± 5	−16 ± 5	...	...
2001 Jan 26.................................	85 ± 5	−32 ± 6	51 ± 4	−11 ± 4	76 ± 5	−16 ± 9	...	...
2003 Jan 2...................................	90 ± 2	−76 ± 8	...	...	...	...	...	...
2003 Jan 3...................................	99 ± 2	−70 ± 6	...	...	...	...	...	...

Notes.—EWs and FWZIs are in units of angstroms. The EWs are the mean of the values obtained for the individual profiles and the uncertainties correspond to the standard deviation. The uncertainties in the FWZIs were estimated by looking at the scatter in the values when selecting different wavelength intervals to set the local continuum level.

during quiescence. In addition, the averaged Hα profiles during the decline to quiescence show long-term changes in the relative intensity of the red and blue peaks, a fact previously reported by Zurita et al. (2002) and also observed during outburst (Torres et al. 2002b). During quiescence the peaks of the line are slightly asymmetric.

6. THE TIME-RESOLVED Hα LINE PROFILE

In order to study the orbital variations in the Hα emission-line profile, we first determined the EWs for the individual spectra on those nights with good orbital phase coverage. The resultant Hα EWs are plotted as functions of the orbital phase in Figure 1. During 2001 January 26, the EW reaches maximum at orbital phase 0.1 and no obvious minimum is observed. During 2003 January 2/3, the Hα EWs display a maximum at phase 0.5. The plot also shows that the EW is significantly higher around phase 0.5 for the first night than for the second night. The variations are unlikely to be caused by the ellipsoidal modulation in the continuum of the secondary star, since one would expect to see two equal minima in the EWs at phases 0.25 and 0.75, corresponding to the two maxima in the ellipsoidal modulation. The variations more probably represent intrinsic changes in the Hα line flux with orbital phase.

The top panels in Figure 3 show the evolution of the Hα profile with orbital phase in the form of trailed spectrograms. They also illustrate the prominent long-term changes in the velocity shifts relative to the rest wavelength of the line and in the asymmetry of the peak intensities (§ 5). Looking to the panels, it is possible to trace the narrow emission components present in the double-peaked line profiles. During 2000 December 29, a sharp emission component is visible at orbital phases 0.3–0.7 that crosses from red to blue at phase ∼0.4. On

TABLE 3
Fits to the Hα Line Profile

Date (UT)	V_b (km s^{-1})	V_r (km s^{-1})	$V_r - V_b$ (km s^{-1})	$(V_b + V_r)/2$ (km s^{-1})
2000 Dec 4	−1163 ± 34	664 ± 14	1827 ± 37	−250 ± 18
2000 Dec 24	−644 ± 16	1021 ± 23	1665 ± 28	188 ± 14
2000 Dec 29	−651 ± 8	1120 ± 17	1771 ± 19	234 ± 9
2001 Jan 26.......	−1134 ± 12	627 ± 7	1761 ± 14	−254 ± 7
2003 Jan 2.........	−952 ± 6	811 ± 8	1763 ± 10	−71 ± 5
2003 Jan 3.........	−1009 ± 6	823 ± 8	1832 ± 10	−93 ± 5

Notes.—V_b and V_r designate the positions (shifts) with respect to the rest wavelength of the line of the blue and red peaks, respectively. The uncertainties were calculated after scaling the error bars to give $\chi_\nu^2 = 1$.

2001 January 26 the line profile shows an emission component in the phase interval 0.7–0.9 that crosses from blue to red at phase ∼0.9. During 2003 January 2/3 an emission component crosses zero velocity from red to blue at around phase 0.5. Because of the gap around phase 0.0 in the orbital phase coverage for the latter epoch, it is not possible to know whether the narrow component is observable at all orbital phases.

Since the narrow components in the emission-line profiles are weak and show a complex behavior, a multi-Gaussian fit to each individual spectrum will render poor information about their origin. However, we can gain insight into the Hα-emitting regions in XTE J1118+480 by using the Doppler tomography technique (Marsh & Horne 1988). This technique reconstructs the brightness distribution of the binary system in velocity space, allowing us to localize the emission structures that are not easily recognizable in the individual spectra. We use the maximum entropy method (MEM) of building the tomograms on those nights with orbital phase covering at least half an orbital cycle and with good spectral resolution: 2000 December 29, 2001 January 26, and 2003 January 2/3. The bottom panels in Figure 3 display the derived MEM tomograms with the theoretical path of the gas stream and the Keplerian velocities of the disk along the stream for a radial velocity semiamplitude of the companion star of $K_2 = 709$ km s^{-1} (§ 3) and a mass ratio $q = 0.037$ (Orosz 2001).

During the approach to quiescence, enhanced emission in the $-V_X$, $+V_Y$ (top left) quadrant, together with the emission arising from the rotating accretion disk, is easily recognizable in the Doppler images. The location of the former emission, halfway between the theoretical disk and gas stream kinematic paths, is similar to that observed in the Balmer and He II λ4686 maps during outburst (Torres et al. 2002b). However, now there is a greater overlap between this region and the theoretical trajectories. On 2000 December 29, a bright spot is present between both theoretical paths at $(0.5 \pm 0.1)R_{L_1} = (0.4 \pm 0.1)a$, where R_{L_1} is the distance of the compact object from the inner Lagrangian point and a the binary separation. The position was determined by using lines passing through points in the theoretical paths at equal distance from L$_1$. On 2001 January 26 a bright spot is again present, but now it is approximately placed on the ballistic trajectory of the gas stream at $(0.77 \pm 0.06)R_{L_1} = (0.61 \pm 0.05)a$. Finally, note the enhanced emission in the $+V_X$, $-V_Y$ (bottom right) quadrant for both tomograms. Its origin is discussed in the next section.

The tomogram computed during quiescence shows no clear evidence of emission from a bright spot on the ringlike distribution of the accretion disk. An emission component
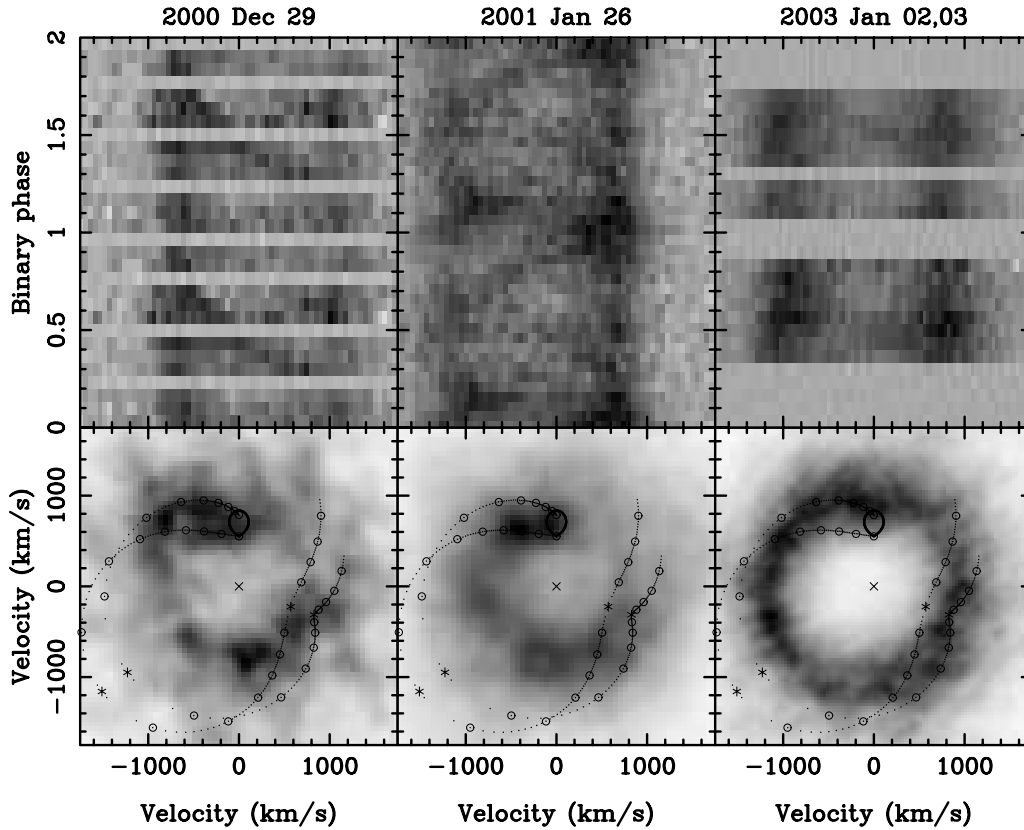
FIG. 3.—*Top*: Trailed spectrograms of Hα. Empty strips represent gaps in the phase coverage. For the sake of clarity, for 2000 December 29 and 2001 January 26 the same cycle has been plotted twice. For 2003 January, the bottom and top halves of the spectrogram are data from January 2 and 3, respectively. *Bottom*: Computed MEM Doppler maps. For 2003 January 2/3, we show the tomogram obtained by combining the data acquired during both nights. The Roche lobe of the secondary star, the predicted velocities of the gas stream (*bottom curve*) and of a Keplerian disk along the stream (*top curve*) are plotted. Distances in multiples of $0.1R_{L1}$ are marked along both curves with open circles. The center of mass of the system is denoted by a cross. [*See the electronic edition of the Journal for a color version of this figure.*]

crossing the double-peaked profile is evident in the trailed spectra, and therefore, it must be reflected in the tomogram at a position defined by the amplitude and phase of its modulation. In order to find its counterpart in the tomogram, we subtracted the azimuthally symmetric part of the map. This was obtained by taking the median of the image values within annuli centered on the center of symmetry of the ring emission, which falls at approximately $(-100, 0)$ km s^{-1} rather than $(0, -K_1)$. Figure 4 shows the result of the subtraction. We can see that the core of the residual emission is situated near the predicted Roche lobe of the secondary. The spread is approximately consistent with the combined effect of the finite spectral resolution (110 km s^{-1}) and orbital phase smearing (ranging from 20 to 270 km s^{-1}).

7. DISCUSSION

From spectroscopic observations of XTE J1118+480 during its approach to quiescence, Zurita et al. (2002) found that the variability in the centroid of the nightly averaged Hα profile was consistent with a periodic modulation of 26 days (half of the 52 day precession period for the accretion disk implied by the superhump period), although a 52 day periodicity was not ruled out. When we combine our centroid measurements obtained for Hα during approach to quiescence (Table 3) with those of Zurita et al., a modulation on the precession period is definitely favored and the 26 day periodicity is ruled out (Fig. 5). The centroids measured for 2003 January 2/3 (Table 3) are also displaced with respect to the systemic velocity, which
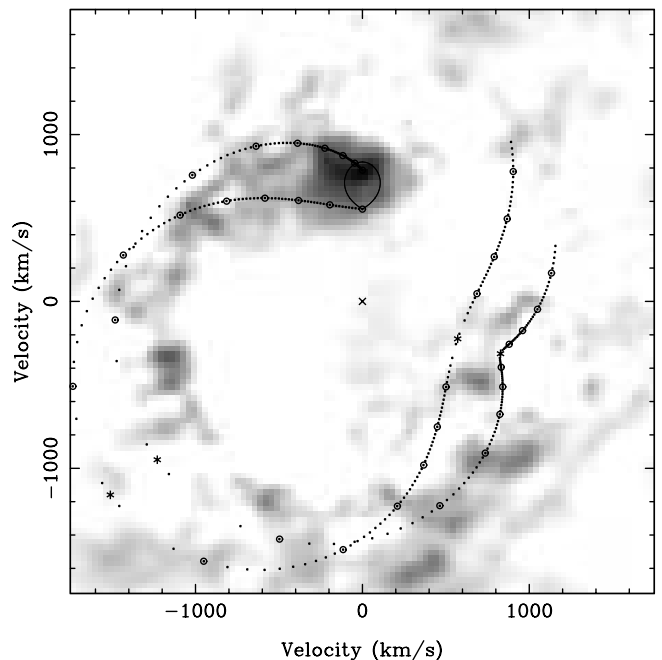

FIG. 4.—2003 January 2/3 Doppler image of Hα after subtraction of the axisymmetric part of the emission (see text for details). [*See the electronic edition of the Journal for a color version of this figure.*]
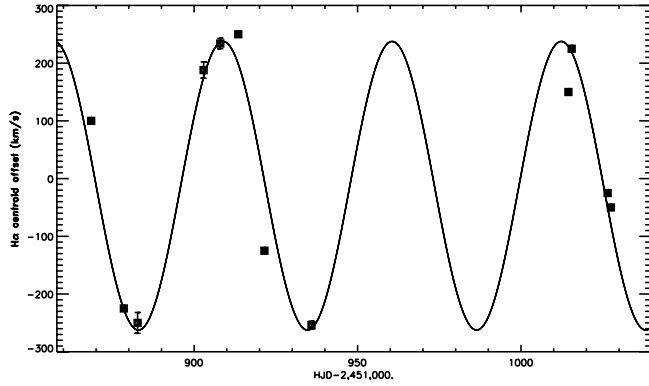
FIG. 5.—Changing centroid of the Hα emission line during approach to quiescence. The velocity points without errors have been extracted from Fig. 5 of Zurita et al. (2002). The best-fit sine wave ($P \sim 52$ days) is also shown.

suggests that the accretion disk continues precessing during true quiescence. This is possible only if the outer disk radius is large enough to reach or exceed the 3 : 2 resonance tidal instability. By using the Hα mean peak-to-peak separation (Δv) and the semiamplitude of the secondary, we estimate an outer radius of $R_d/a = (1 + q)(2K_2/\Delta v)^2 = 0.66 \pm 0.05$ (see, e.g., Dubus et al. 2001). This is a value definitely larger than the 3 : 2 resonance radius $r_{32}/a(q) = 0.47$ (Whitehurst & King 1991) and comparable to the expected disk tidal truncation radius $R_T/a = 0.6/(1 + q) = 0.58$ (Warner 1995). In addition, the hot spot in the 2001 January 26 tomogram is located at a position consistent with the predicted outer disk radius.

Before we continue with the discussion of the Doppler maps obtained in the previous section, it is important to stress that the Doppler tomography technique assumes (in particular) that all the emitting regions corotate in the binary and that the flux from any of these regions is constant with time. These assumptions might not be fulfilled in a precessing eccentric disk during the course of a single orbit (Foulkes et al. 2004), and therefore, the results obtained from the tomograms must be interpreted with caution. Bearing this in mind, we see in the tomograms for 2000 December 29 and 2001 January 26 emission from the hot spot and the gas stream, illustrating that mass transfer from the donor star has continued during the approach of the system to quiescence. They also show changes in the position of the hot spot (see § 6). It is interesting to note here that the changes observed in the position of the hot spot may be modulated with the precession period because of the varying geometry of the elliptic disk. On the other hand, the emission in the bottom right quadrant may be interpreted as arising from an overflowing gas stream that, after the first impact, intersects again the disk close to phase 0.5 (see, e.g., Kunze et al. 2001) or as arising from a nonuniform brightness distribution across the disk. In the latter case, the formation of a region of enhanced density (temperature) in the disk may be caused by tidal forces from the companion star (see, e.g., Steeghs & Stehle 1999). It is clear from the long-term variations in the centroid and peak intensities of the Hα profile that the disk in XTE J1118+480 continues to experience the tidal stresses from the companion star.

The residual Hα image obtained by subtracting the symmetric part from the 2003 January 2/3 Doppler image uncovers emission concentrated toward the expected position of the secondary star. Hα emission from the hot spot or gas stream is not detected, a fact that points to a decrease or pause in the mass transferred from the donor star to the accretion disk. A

similar scenario was suggested to explain the quiescent Hα tomograms of Nova Muscae 1991 (Casares et al. 1997) and Centaurus X-4 (Torres et al. 2002a), which show the same pattern (secondary's emission present/absence of hot spot). In order to constrain the nature of the Hα emission from the secondary star, we isolated the narrow-line component of the line profile as follows: first, an accretion disk profile was created by averaging all the target spectra in the observer's rest frame. Next, 17 copies of the simulated disk profile were shifted to the rest frame of the secondary star at the times of the individual target spectra and then averaged using the same weights as in the first step of the procedure. Finally, the resultant profile was subtracted from the Doppler-corrected Hα averaged profile of XTE J1118+480. This left us with a residual with an EW = 1.0 ± 0.5 Å, which represents 1% of the total Hα emission. For an R-band quiescent magnitude of 18.6 and a distance of 1.8 kpc, and assuming a secondary with a stellar radius equal to the volume radius of its Roche lobe ($R_2 = R_L(2) = 0.15a$, with $a = 2.5$ $R_\odot$ for $M_1 = 7$ $M_\odot$ and $i = 80°$), we derive from the EW of the Hα residual an Hα flux at the surface of the star ($F_{H\alpha}$) of 3×10^6 ergs cm^{-2} s^{-1}.

Does X-ray irradiation power the Hα emission from the donor star? The intrinsic quiescent X-ray luminosity in the 0.3–7 keV band was estimated by McClintock et al. (2003) to be $L_X \approx 3.5 \times 10^{30}$ ergs s^{-1}. The implied X-ray irradiation at the secondary star is then $F_X = L_X/(4\pi a^2) = 9 \times 10^6$ ergs cm^{-2} s^{-1}, which can account for the Hα emission if at least 30% of the incident X-ray flux is reprocessed to Hα photons. We can obtain a rough estimate of the likely fraction of the X-ray luminosity converted to Hα photons by assuming that the Hα emission line observed in X-ray bright LMXBs is due completely to X-ray reprocessing in the disk. Then,

$$L_{H\alpha} \sim \frac{EW}{(7000-3000 \text{ Å})} L_{opt} \sim 10^{-6} L_X,$$

where we have taken into account that for LMXBs the averaged optical to X-ray luminosity is $L_{opt}(3000-7000 \text{ Å})/L_X$ (2–11 keV) ~ 0.002 (van Paradijs & McClintock 1995) and the EW of the Hα emission line is of the order of a few Å (see, e.g., Shahbaz et al. 1996; Torres et al. 2002b). Therefore, we find it improbable that the X-ray irradiation could be the source of the Hα emission in the secondary star.

A chromospherically active secondary is an alternative explanation to the Hα emission. We can compare the above estimates with the results reported by Soderblom et al. (1993) for rapidly rotating dwarfs in the Pleiades. In order to compare the EW of the Hα residual, we first subtracted the underlying Hα profile of the secondary star from the Hα residual by using the dwarf templates and taking into account the veiling from the accretion disk (§ 4). This operation yielded a corrected EW of 3 Å. By looking at Table 6 of Soderblom et al. we find that the Hα emission in the companion of XTE J1118+480 is comparable in strength to that observed in some of the K dwarfs in their sample. For example, for the K7 V star listed as k403, EW = 3.41 Å and $F_{H\alpha} = 6.12 \times 10^6$ ergs cm^{-2} s^{-1}.

7.1. Comparison of XTE J1118+480 and GRO J0422+32

Among the black hole XRNe, GRO J0422+32 (Nova Per 1992; $P = 5.1$ hr) has the orbital period closest to that of XTE J1118+480 and has also exhibited superhumps during the 1992 outburst (O'Donoghue & Charles 1996 and references therein), suggesting a precessing accretion disk in the system in accordance with its low mass ratio ($q = 0.12^{+0.08}_{-0.07}$; Harlaftis et al.

TABLE 4
ASYMMETRIES IN THE AVERAGED DOUBLE-PEAKED Hα PROFILE OF GRO J0422+32

Nights Averaged	Net Exposure (hr)	Stronger Peak	Comments	References
1993 Oct 10	5.3	Blue	Decay to quiescence after August minioutburst	1
1993 Oct 12	5.3	Blue	. . .	. . .
1993 Dec 9	6	Red	Maximum December minioutburst	2
1993 Dec 10	5	Red	. . .	. . .
1993 Dec 16–19	~11	Blue	Initial decline of minioutburst	3
1994 Nov 5–7	>14.5	Blue	Quiescence	4
1995 Jan 26	4.9	Red	Quiescence	5

REFERENCES.—(1) Garcia et al. 1996; (2) Fig. 5d in Callanan et al. 1995; (3) Fig. 2 in Casares et al. 1995; (4) Fig. 2 in Orosz & Bailyn 1995; (5) Fig. 1 in Harlaftis et al. 1999.

1999). In contrast, the decay to quiescence was interrupted by two minioutbursts in 1993 August and December. Motivated by the similarities between these systems, we have searched the literature for evidence of a precessing accretion disk from the Hα emission line of GRO J0422+32. We have found that asymmetries in the double peaks of the averaged line profile have been observed (see Table 4), which we suggest are most likely due to a precessing accretion disk. In addition, the centroid of the emission profiles should also vary if the disk is precessing. This may be reflected in the Hα systemic velocity of $+142 \pm 4$ km s^{-1} obtained by Garcia et al. (1996), in comparison with the secondary's systemic velocity of $\gamma = 11 \pm 8$ km s^{-1} (Harlaftis et al. 1999). Note that Filippenko et al. (1995) found an Hα systemic velocity of 26.0 ± 1.6 km s^{-1} by combining data obtained on 1994 November 8/9 and 1995 January 26/27. Qualitatively, the Hα and He II $\lambda4686$ trailed profiles in Fig. 6 of Casares et al. (1995) are redshifted by ~100 km s^{-1}. We suggest that these variations are also associated with a precessing disk. Future spectroscopic monitoring of XRNe in outburst and decline will enable us to confirm unambiguously the relation between the long-term variations in the line profiles and the precession of the accretion disk.

8. SUMMARY

We have presented comprehensive optical spectroscopy of the XRN XTE J1118+480 from 2000 December to 2003 January. From the analysis of the absorption line spectrum, we have established an orbital period of $P = 0.1699339 \pm 0.0000002$ days and a radial velocity semiamplitude of the secondary of $K_2 = 709 \pm 7$ km s^{-1}. The implied updated mass function is $f(M) = 6.3 \pm 0.2$ $M_{\odot}$. Inspection of the averaged spectrum of XTE J1118+480 in the rest frame of the secondary star exhibits numerous photospheric features typical of a secondary of spectral type K–M. Our analysis of the absorption features suggests that the system has reached true quiescence, with the companion star contributing $\sim55\%$ of the total flux over the range $\lambda\lambda5800$–6400. The long-term variations in the centroid of the Hα profile during the decline to quiescence show a periodicity of ~52 days and an amplitude of 250 km s^{-1}. They are interpreted as due to a precessing accretion disk. Comparison between two tomograms of the Hα line profile during the approach of the system to quiescence show a hot spot whose position varies. The change in the hot spot location may be related to the changes in the gas stream impact site at the edge of the disk as it precesses. During quiescence, both hot spot and gas stream are not present, which points to a decrease or cessation of the mass transfer from the secondary. Hα emission is detected near the location of the secondary and is most probably due to chromospheric activity.

REFERENCES

Callanan, P. J., et al. 1995, ApJ, 441, 786
Casares, J., Charles, P. A., & Marsh, T. R. 1995, MNRAS, 277, L45
Casares, J., Martín, E. L., Charles, P. A., Molaro, P., & Rebolo, R. 1997, NewA, 1, 299
Dubus, G., Kim Rita, S. J., Menou, K., Szkody, P., & Bowen, D. V. 2001, ApJ, 553, 307
Filippenko, A. V., Matheson, T., & Ho, L. C. 1995, ApJ, 455, 614
Foulkes, S. B., Haswell, C. A., Murray, J. R., & Rolfe, D. 2004, MNRAS, 349, 1179
Frontera, F., et al. 2003, ApJ, 592, 1110
Garcia, M., Brown, W., Pahre, M., McClintock, J., Callanan, P., & Garnavich, P. 2000, IAU Circ. 7392
Garcia, M. R., Callanan, P. J., McClintock, J. E., & Zhao, P. 1996, ApJ, 460, 932
Harlaftis, E. T., Collier, S., Horne, K., & Filippenko, A. V. 1999, A&A, 341, 491
Haswell, C. A., Hynes, R. I., King, A. R., & Schenker, K. 2002, MNRAS, 332, 928

Hynes, R. I., Mauche, C. W., Haswell, C. A., Shrader, C. R., Cui, W., & Chaty, S. 2000, ApJ, 539, L37
Kunze, S., Speith, R., & Hessman, F. V. 2001, MNRAS, 322, 499
Marsh, T. R., & Horne, K. 1988, MNRAS, 235, 269
Marsh, T. R., Robinson, E. L., & Wood, J. H. 1994, MNRAS, 266, 137
Martín, E. L., Casares, J., Molaro, P., Rebolo, R., & Charles P. 1996, NewA, 1, 197
Martín, E. L., Rebolo, R., Casares, J., & Charles, P. A. 1994, ApJ, 435, 791
McClintock, J. E., Garcia, M. R., Caldwell, N., Falco, E. E., Garnavich, P. M., & Zhao, P. 2001b, ApJ, 551, 147L
McClintock, J. E., Narayan, R., Garcia, M. R., Orosz, J. A., Remillard, R. A., & Murray S. S. 2003, ApJ, 593, 435
McClintock, J. E., & Remillard, R. A. 2004, in Compact Stellar X-Ray Sources, ed. W. H. G. Lewin & M. van der Klis (Cambridge: Cambridge Univ. Press), in press (astro-ph/0306213)
McClintock, J. E., et al. 2001a, ApJ, 555, 477
Mirabel, I. F., Dwarawan, V., Mignani, R. P., Rodrigues, I., & Guglielmetti, F. 2001, Nature, 413, 139

O'Donoghue, D., & Charles, P. A. 1996, MNRAS, 282, 191
Orosz, J. A. 2001, Astron. Telegram, 67, 1
Orosz, J. A., & Bailyn, C. D. 1995, ApJ, 446, L59
Remillard, R., Morgan, E., Smith, D., & Smith, E. 2000, IAU Circ. 7389
Rhodes, C. E., & Ruffini, R. 1974, Phys. Rev. Lett., 32, 324
Shahbaz, T., Smale, A. P., Naylor, T., Charles, P. A., van Paradijs, J., Hassall,
    B. J. M., & Callanan, P. 1996, MNRAS, 282, 1437
Soderblom, D. R., Stauffer, J. R., Hudon, J. D., & Jones, B. F. 1993, ApJS,
    85, 315
Steeghs, D., & Stehle, R. 1999, MNRAS, 307, 99
Tanaka, Y., & Shibazaki, N. 1996, ARA&A, 34, 607
Torres, M. A. P., Casares, J., Martínez-Pais, I. G., & Charles P. A. 2002a,
    MNRAS, 334, 233

Torres, M. A. P., et al. 2002b, ApJ, 569, 423
Uemura, M., et al. 2000a, IAU Circ. 7418
———. 2000b, PASJ, 52, L15
van Paradijs, J. 1998, in The Many Faces of Neutron Stars, ed. R. Buccheri,
    J. van Paradijs, & M. A. Alpar (Dordrecht: Kluwer), 279
van Paradijs, J., & McClintock, J. E. 1995, in X-Ray Binaries, ed. W. H. G.
    Lewin, J. van Paradijs, & E. P. J. van den Heuvel (Cambridge: Cambridge
    Univ. Press), 107
Wagner, R. M., Foltz, C. B., Shahbaz, T., Casares, J., Charles, P. A., Starrfield,
    S. G., & Hewett, P. 2001, ApJ, 556, 42
Warner, B. 1995, Cataclysmic Variables (Cambridge: Cambridge Univ. Press)
Whitehurst, R., & King, A. J. 1991, MNRAS, 249, 25
Zurita, C., et al. 2002, MNRAS, 333, 791